Chalcogenide Letters Vol. 2, No. 8, August 2005, p. 77 - 82

SMD PACKAGED ZnSSe ULTRA-VIOLET SCHOTTKY PHOTODETECTORS WITH HIGH DETECTIVITY

L. S. Mak, S. K. Chan, G. K. L. Wong, I. K. Sou*

Department of Physics, The Hong Kong University of Science and Technology
Clear Water Bay, Kowloon, Hong Kong, People' China

We report the 1/f noise and shot noise studies on molecular beam epitaxy (MBE)-grown ZnSSe UV detectors packaged in SMD leadframes for three detectors with different thicknesses of the active layer and the top electrode pad. The highest onset of reverse bias for the appearance of 1/f noise is -27.5V and the highest dark resistances at zero bias is R_0 = 3.7 X $10^{13}\Omega$. The observed difference in their noise performance implies that the increase of the thicknesses of both the active layer and the top electrode pad can significantly lower the noise levels and in turn lead to higher detectivity. The best detectivity achieved is 8.75×10^{13} $cmHz^{1/2}W^{-1}$ in a detector with an active layer of 5000 Å and a top electrode pad of Cr (50Å) / Au (8000Å).

1. Introduction

Ultra-violet photodetectors respond only to ultraviolet light with high discrimination against visible and infrared radiation can find applications in areas such as fire detection, flame combustion control, UV astronomy, industrial and medical applications as well as in a number of personal health care consumer products. In recent years, there has been increasing interest in developing GaAlN alloy, SiC, diamond, and a number of wide bandgap II-VI thin film based visible-blind and solar-blind UV detectors [1].

The noise characteristics and detectivity of photodetectors reflect their ultimate limit on small-signal detection. A previous article by Yang et al. [2] reported that a thermally limited specific detectivity as high as $8 \times 10^{14} cmHz^{1/2}W^{-1}$ can be achieved in their AlGaN/GaN p-i-n photodetector array. The most recent report on the noise characterization of GaN-based UV detectors was given by H. Jiang et al. [3] who reported that GaN Schottky photodiodes using oxidized IrNi Schottky contact can achieve a thermally limited specific detectivity as high as $5.8 \times 10^{15} cmHz^{1/2}W^{-1}$, however the background limited contribution based on noise spectral density measurement has not been studied. On the other hand, Vigué et al. [4] presented the noise measurement on ZnMgBeSe Schottky barrier UV diodes and reported a detectivity of $2 \times 10^{12} cmHz^{1/2}W^{-1}$. In the past few years, we have successfully fabricated a novel $ZnS_{1-x}Se_x$-based Schottky barrier UV detector system grown on closely lattice-matched GaP substrates, which offer a cutoff wavelength tunable between 340 and 400nm [5]. These detectors exhibit external quantum efficiency as high as 50%, response time as fast as 1.2 ns for an active area of 0.16 mm^2, visible rejection power of more than 4 orders. Recently, we have also demonstrated $ZnMg_{1-y}S_y$ UV detectors with even shorter cut-off wavelengths for solar-blind applications [6]. We have performed detailed noise measurements on a set of $ZnS_{0.58}Se_{0.42}$ UV photodiodes [7]. Based on the combined electrical and noise measurements including 1/f noise studies, the best specific detectivity achieved for detectors packed in TO cans is as high as $7.1\times10^{14} cmHz^{1/2}W^{-1}$. Since most applications in UV detection technology require a compact packaging, we have recently developed a packaging technology based on SMD (surface mounted devices) design for a number of consumer products such as watches, personal UV monitor and UV teaching kits. In this article, we report the noise characterization and detectivity measurement for $ZnS_{0.85}Se_{0.15}$ UV detectors packaged in SMD leadframes with focus on the dependence of their performance on the thicknesses of the active layer and the electrode pad.

* Corresponding author: phiksou@ust.hk

2. Experimental

The $ZnS_{0.85}Se_{0.15}$ layers of the detectors were grown on n^+-GaAs substrates by the molecular beam epitaxy (MBE) technique using a VG V80H growth chamber. At first, a 1000Å thick $ZnS_{0.85}Se_{0.15}$:Al layer was grown on the substrate, which is common for the three detectors used in this study. This heavily doped II-VI buffer layer is useful to limit the propagation of misfit dislocation near the substrate interface. Following the growth of the buffer layer, an intrinsic $ZnS_{0.85}Se_{0.15}$ layer was grown to act as the active layer. The thicknesses of the active layer of Detector 1 and 2 are both of 2000 Å, while that of Detector 3 is 5000Å.

Standard photolithographic technique was used to define mesa structures to fabricate micro-devices on the sample wafer. These involve the thermal evaporation of a 100 Å-Au thin film as the top transparent electrode followed by the deposition of a thick Cr/Au layer in the center of the top electrode to form a bonding pad on the active layer. The bonding pad of Detector 1 consists of Cr (50Å) / Au (2000Å), while that of Detector 2 and 3 are of Cr(50Å) / Au (8000Å) with the Cr layer making direct contact with the surface of the active layer to assure good adhesion. Then, the wafers were diced into devices each with active area of $0.04mm^2$. Sliver paint was used to attach the die to a SMD leadframe thus forming an ohmic contact at the back of the n^+-GaAs substrate. Finally, the die detectors were wire-bonded and protected by UV-transparent epoxy.

The 1/f noise characteristics of the detectors were measured using an SR-570 low noise current pre-amplifier and an SR-760 spectrum analyzer. The detector and the dry battery for providing reverse bias voltage were shielded in a grounded aluminum box to reduce the background noise. In order to measure the noise of the detectors, the background noise must first be determined. The background noise included the noise from the equipment and the surroundings. It can be estimated by replacing the detector being studied with a capacitor having a capacitance close to that of the detector. The background noise of the set up was found to be about $10^{-26}A^2/Hz$. The low frequency (1 to 100 Hz) noise measurements were taken under reverse bias starting from 3V.

The I-V characteristics of the detectors was measured using a Keithley 237 voltage/current source unit that is able to measure the current passing through the photodiode at different forward bias and reverse bias. The data were collected by a computer program for controlling the instruments. A Hewlett Packard (HP) 16442A test fixture was used as a screening box, combining with the use of Keithley 237 voltage/current source unit, this system can sense current as low as a few tens of femto amperes.

3. Results and discussion

The noise spectral characterization revealed that the onset reverse bias for the appearance of detectable noise is very different among the three detectors being studied. They are -3V, -9V and -27.5 V for Detector 1, 2 and 3, respectively. Figure 1 shows the noise spectral density curves of Detector 1 (at -3V), 2 (at -9V) and 3 (at -27.5V) respectively, together with the measured background noise spectrum. Each of the noise spectra can be well fitted with a straight line of the form of $N_{1/f} = A/f^{\beta}$. The best fitted parameter A and β were determined for the calculation of total 1/f noise within the bandwidth of the detectors based on the equation as shown below:

$$I_{1/f}^2 = A[1 + \int_1^B (1/f^{\beta})df] \quad (1)$$

where B is the bandwidth of the detector, which was taken as 300MHz as determined in our previous work [7]. The fitting parameters and the calculated total 1/f noise of the three detectors at their onset reverse bias are listed in Table 1.

Table 1. Fitted values of parameter A and β and the total 1/f noise for the three detectors.

Reverse bias	A (A^2)	β	Total 1/f noise (A^2)
-3V (Detector 1)	7.62×10^{-19}	0.76	3.41×10^{-16}
-9V (Detector 2)	6.85×10^{-18}	1.58	1.87×10^{-17}
-27.5V (Detector 3)	3.70×10^{-18}	1.41	1.27×10^{-17}

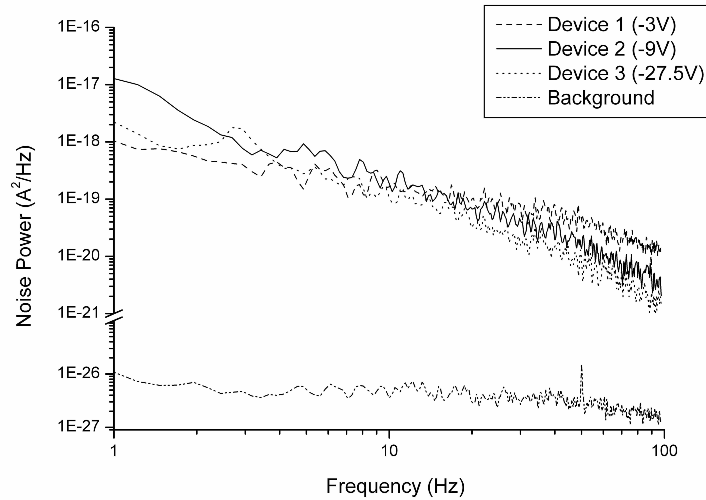

Fig. 1. The spectrum of low frequency noise power of Detector 1, Detector 2 and Detector 3 with bias of -3V, -9V and -27.5V respectively.

The measured I-V characteristics of Detector 1, 2 and 3 are shown in Fig.2a, Fig.2b and Fig. 2c respectively. For the I-V characteristics of detector 3, the data from 0 to -1.5V were below the detectable limit (10fA) of the voltage/current source unit. All three detectors show a very good rectified behavior as expected from a Schottky barrier. Their dark resistances at zero bias were determined using Collins et al.'s approach as described below. Curve fitting was performed using exponential fits to both the forward and reverse bias curves. The constants obtained from curve fitting were then used in the following equation:

$$I = a(\exp(b\times V)-1)+c(\exp(d\times V)-1) \quad (2)$$

where a and b are the coefficients from the reverse bias fit and c and d are the coefficients from the forward bias fit. The dark resistance R_0 was estimated by taking the inverse derivative of the fit at zero bias:

$$1/R_0 = (dI/dV)\big|_{V=0}, \quad (3)$$

The fitted dark resistances at zero bias and the measured dark currents at different bias of the three detectors were shown in Table II.

The shot noise power of a detector when it is operated at zero bias can be calculated using its dark resistance and the following equation,

$$I^2_{shot} = 4kTB/R_0 \quad (4)$$

where R_o the dark resistance, k is is the Boltzmann constant, T is the absolute temperature and B is the bandwidth of the detector. The shot noise power of a detector at reverse bias can be obtained by,

$$I^2_{shot} = 2I_{dc}qB \quad (5)$$

where I_{dc} is the DC current passing through the detector at the operating bias which is equivalent to the dark current listed in Table II. The calculated shot noise powers of the three detectors being studied at different bias are also shown in this table.

For both zero bias and under reverse bias operation, the noise equivalent power and the specific detectivity of the detectors are calculated as,

$$NEP = \sqrt{I^2_{shot} + I^2_{1/f}} / R, \qquad D^* = \sqrt{A \times B} / NEP \quad (6)$$

where R is the responsivity (the responsivity data shown in Table II are estimated from our previous work [7]) and A is the active area of the detectors. The NEP values were calculated for the bandwidth B at 300 MHz. The detector parameters and the calculated NEP and D^* at 330nm in wavelength for the three detectors are listed in Table II. The best detectivity results from Detector 3 at zero bias, and it reaches 9.15×10^{13} $cmHz^{1/2}W^{-1}$, which is among the best of UV detectors reported so far.

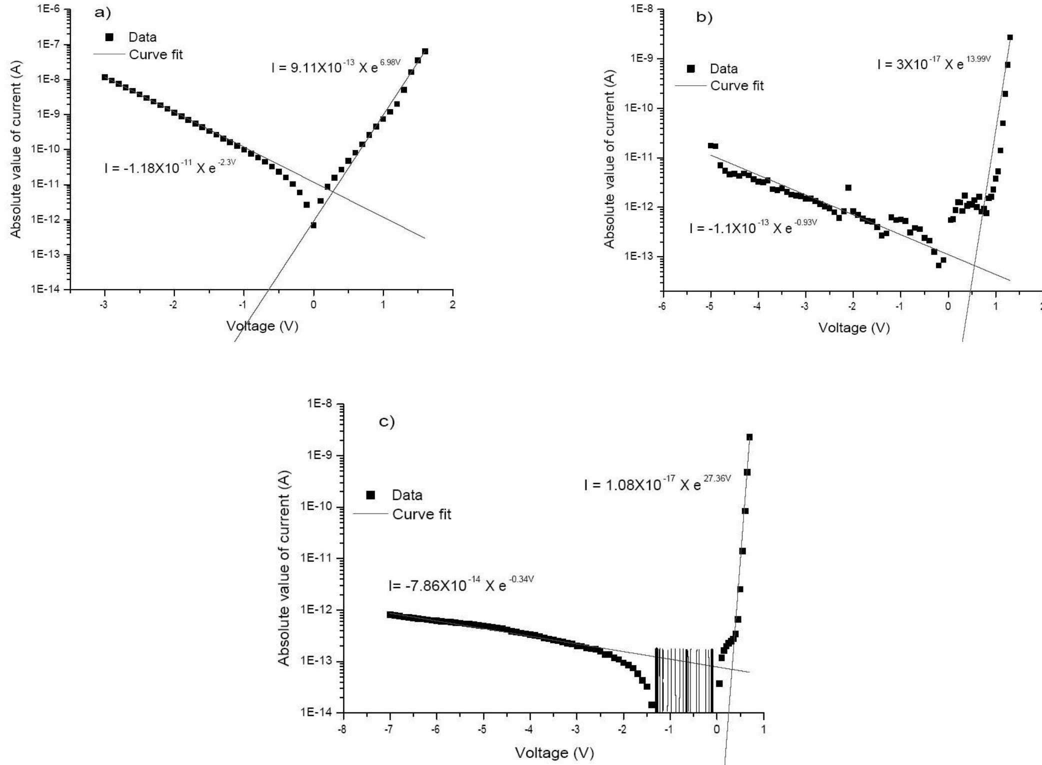

Fig. 2. Log plot of the absolute value of I-V data of a) Detector 1, b) Detector 2 and c) Detector 3 with exponential fit.

Table 2. Performance data of the three detectors.

Device	Bias voltage (V)	Dark resistance (Ω)	Dark Current (A)	Shot Noise (A^2)	Total 1/f Noise (A^2)	Responsivity at 330nm (A/W)	NEP for 300MHz bandwidth (W)	Detectivity ($cmHz^{1/2}W^{-1}$)
Detector 1	0	R_0 = 2.98 X 10^{10}	-	1.67 X 10^{-22}	-	0.093	1.39 X 10^{-10}	2.48 X 10^{12}
	-3	-	1.18 X 10^{-8}	1.13 X 10^{-18}	3.41 X 10^{-16}	0.163	1.13 X 10^{-7}	3.05 X 10^{9}
	-5	-	-	-	-	-	-	-
Detector 2	0	R_0 = 1.03 X 10^{13}	-	4.82 X 10^{-25}	-	0.093	7.47 X 10^{-12}	4.61 X 10^{13}
	-3	-	1.51 X 10^{-12}	1.45 X 10^{-22}	-	0.163	7.29 X 10^{-11}	4.73 X 10^{12}
	-5	-	1.76 X 10^{-11}	1.69 X 10^{-21}	-	0.175	2.35 X 10^{-10}	1.47 X 10^{12}
Detector 3	0	R_0 = 3.7 X 10^{13}	-	1.34 X 10^{-25}	-	0.093	3.94 X 10^{-12}	8.75 X 10^{13}
	-3	-	2.02 X 10^{-13}	1.94 X 10^{-23}	-	0.163	2.70 X 10^{-11}	1.28 X 10^{13}
	-5	-	4.93 X 10^{-13}	4.73 X 10^{-23}	-	0.175	3.93 X 10^{-11}	8.77 X 10^{12}

From a close inspection of Fig. 2 and Table II, one can see that Detector 2 shows a much better performance in 1/f noise level, short noise level and detectivity as compared to that of Detector 1, and Detector 3 is the best among all three detectors. These results are also in good agreement with their onset of reverse bias for the appearance of detectable noise as mentioned in the beginning of this section. We believe that the observed difference in their performance is attributed to the difference among their structural design as stated in the previous section. The increase of both the thicknesses of the bonding pad and the active layer can lower the 1/f and short noise levels and thus results higher detectivity. It is believed that a thicker bonding pad can reduce the damage caused by the wire bonding process and a thicker active layer can reduce the leakage current that flows through the lattice mismatch dislocation network located at the interface between the buffer layer and the substrate.

In summary, both the 1/f noise and shot noise characteristics of MBE-grown ZnSSe UV detectors packaged in SMD leadframes were studied. The three detectors used in this study are distinguished in their thicknesses of the active layer and the top electrode pad. We have found that the difference in their performance in terms of the 1/f noise and shot noise seems to indicate that the increase of the thicknesses of both the active layer and the top electrode pad can significantly lower the noise levels. The best detectivity achieved among the SMD packaged devices is 8.75×10^{13} $cmHz^{1/2}W^{-1}$ in a detector with an active layer of 5000 Å and an top electrode pad of Cr (50Å) / Au (8000Å).

Acknowledgement

The MBE growth in this study was carried out at the Zheng Ge Ru Thin Film Physics Laboratory in the Department of Physics of The Hong Kong University of Science and Technology (HKUST). Metallization was performed in the Materials Characterization and Preparation Facilities (MCPF) of HKUST. The work described here was substantially supported by a grant from the Research Grants Council of the Hong Kong Special Administrative Region, China (Project No. HKUST6072/02E).

References

[1] E. Monroy, F. Omnes, F. Calle, Semicond. Sci. Technol. **18**, R33 (2003).
[2] B. Yang, K. Heng, T. Li, C.J. Collins, S. Wang, R.D. Dupuis, J.C. Campbell, M. J. Schurman, I. T. Ferguson, IEEE J. Quan. Elec. **36**, 1229 (2000).
[3] H. Jiang, T. Egawa, H. Ishikawa, YB Dou, CL Shao, T. Jimbo, Electronics Letters **39**, 1604 (2003).
[4] F. Vigue, E. Tournie, J. –P. Faurie, E. Monroy, F. Calle,d E. Munoz, Appl.Phys. Lett. **78**, 4190 (2001).
[5] I. K. Sou, Z. H. Ma,d G. K. L. Wong., Appl. Phys. Lett. **75**, 3707 (1999).
[6] I. K. Sou, M. C. W. Wu, T. Sun, K. S. Wong, G. K. L. Wong, Appl. Phys. Lett. **78**, 1811 (2001).
[7] L. S. Lai, I. K. Sou, C. W. Y. Law, K. S. Wong, Z. Yang, G. K. L. Wong. Optical Materials **23**, 21 (2003).